

Solutions of the Poisson–Nernst–Planck Equations involving Ionization for Characterizing the Influence of Electrode Reactions in a Weak Electrolyte

Yohichi Suzuki and Kazuhiko Seki*

Nanomaterials Research Institute(NMRI),

National Institute of Advanced Industrial Science and Technology (AIST)

AIST Tsukuba Central 5, Higashi 1-1-1,

Tsukuba, Ibaraki, Japan, 305-8565

Abstract

When ions are consumed by electrode reactions, ion mass flows are induced and the ion concentrations near the electrode are lower than those in the bulk phase. As a result, charge neutrality is broken at the electrode surface. Using the Poisson–Nernst–Planck equations, we studied ion concentration profiles and the charge density gradient caused by electrode reactions in weak electrolytes without assuming charge neutrality. In weak electrolytes, only a small fraction of molecules are ionized in the bulk. Ion concentration profiles depend on not only ion transport but also ionization of molecules. We took into account ionization of molecules and ion association in weak electrolytes and obtained analytical expressions of electrostatic potential profiles and ion currents. The results were compared with those obtained for strong electrolytes. In strong electrolytes, although the charge density gradient is characterized by the Debye length, ion mass density profiles are considerably long-ranged. We showed that the length scale separation does not hold and charge neutrality is not an acceptable approximation to obtain concentration profiles in certain weak electrolytes. We validate the analytical expressions by comparison with numerical solutions.

I. INTRODUCTION

The Poisson-Nernst-Planck (PNP) equations have been used to describe wide range of transport phenomena from electrons and holes in semiconductors to ions in electrolytes.¹⁻⁸ The conservation of charge for each ion species and electrostatic interactions among charge carriers are treated by the PNP equations in a self-consistent manner. The PNP equations take into account the drift currents due to the electric fields generated by distribution of charge carriers. The effect is important *e.g.* when charge density gradients are generated by electrode reactions: the PNP equations can be applied to obtain concentration profiles and an electro-static potential generated by electrode reactions. Although the PNP equations are useful to study coupled effects between electric fields and charge carrier transports, they are nonlinear and solved mainly by numerical methods. However, for certain cases, approximate analytical solutions have been also obtained.^{2,3,8-12} In bulk neutral electrolytes, concentration profiles can be obtained by assuming charge neutrality to simplify the PNP equations except the regions near the electrode surfaces of the order of the Debye length.^{1-3,8,10,12} For the regions near the electrode surfaces, the charge density characterizing local deviations from charge neutrality can be approximately obtained by linearizing the PNP equations.¹⁻³ In strong electrolytes, the spatial dimensions of concentration gradient can be many orders of magnitude larger than the characteristic length scale of charge density profiles given by the Debye length and the charge neutrality can be safely assumed to obtain concentration profiles except near the electrode surfaces.^{1-4,12} Although ion concentration and electrostatic potential profiles have been calculated without assuming charge neutrality when local equilibrium is realized or broken only by alternative current, charge neutrality assumption is very useful to obtain large scale profiles under direct current for strong electrolytes.

In this paper, we show that the length scale separation does not hold in a certain weak electrolytes. In weak electrolytes, only a small fraction of molecules are ionized in the bulk. Ion concentration profiles depend on not only ion transport but also ionization of molecules. The Nernst-Planck equation is the continuity equation representing the conservation of charge for each ion species, where dissociation and association of ions are not taken into account. For weak electrolytes, the PNP equations have been extended to describe ionization and recombination of ions.^{5,13-21} In the extended PNP (e-PNP) equations, ion concentrations become non-conservative by local dissociation and association of ions

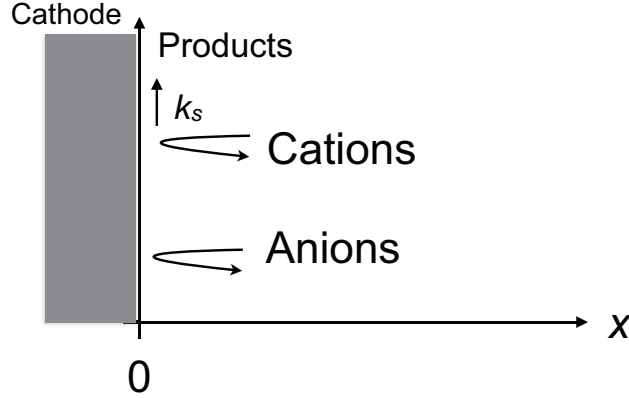


FIG. 1. Sketch of the model of electrode reactions. The distance from the electrode is denoted by x .

in bulk phase. Conventionally, ion concentration profiles in weak electrolytes have been calculated using the e-PNP equations by further assuming charge neutrality as in strong electrolytes.^{5,13-21} The charge neutrality can be assumed to calculate concentration profiles if the characteristic length scales of the concentration profiles are well separated from the length scale of the charge density gradient. Contrary to this expectation, we show that the spatial extent of ion concentration gradient is comparable to that of charge density gradient in 1:1 monovalent weak electrolytes using the e-PNP equations without assuming a priori charge neutrality. Specifically, we consider charge transport induced by electrode reactions in weak electrolytes. Photoelectrochemical (PEC) conversion of water can be an example but the fundamental results apply to other electrode reactions. We obtain analytical expressions for ion concentrations, electrostatic potential profiles, and current densities by linearizing the e-PNP equations. We validate the analytical expressions by comparison with numerical solutions. For comparison, we also show the same parameters in strong electrolytes.

II. THEORY

As shown in figure 1, we considered the thermal motion of cation and anion under Coulombic interactions. The one-dimensional (1D) x -coordinate was introduced by assuming a uniform distribution of ions in the plane parallel to the electrode surface. The origin of the x -coordinate was the electrode surface and the x -coordinate was normal to the electrode surface. The concentration and diffusion constant of cations are denoted as n_+ and D_+ ,

respectively. The concentration and diffusion constant of anions are denoted as n_- and D_- , respectively, while the electric field is denoted as E . Each species moves by electromigration and diffusion. For simplicity, we consider a binary electrolyte (1:1 electrolyte). At a sufficiently large distance L away from the electrode, the electrolyte is neutral. External electric field is not applied and distance to a counter electrode should be larger than L . We consider ion discharge reaction at the electrode followed by product formation. Products of electrode reactions are assumed to be removed. An example is hydrogen evolution reaction by photo-electrocatalytic (PEC) water splitting.^{22,23} When products cover the electrode surface without removal, we need to assume that product formation is the slowest rate determining step. In this case, our approach could be regarded as the quasi-steady state approximation when the surface coverage is much lower than the fraction of uncovered surface.

Ion transport was described by the Nernst–Planck equations and the electric field satisfied the Poisson equation. By taking into account the association and dissociation reactions of ions, the governing equations are given by^{5,13–20}

$$\frac{\partial}{\partial t}n_+ = \frac{\partial}{\partial x}D_+ \left(\frac{\partial n_+}{\partial x} - \frac{eEn_+}{k_B T} \right) + k_a (K_w - n_+n_-), \quad (1)$$

$$\frac{\partial}{\partial t}n_- = \frac{\partial}{\partial x}D_- \left(\frac{\partial n_-}{\partial x} + \frac{eEn_-}{k_B T} \right) + k_a (K_w - n_+n_-), \quad (2)$$

$$\frac{\partial}{\partial x}E(x) = \frac{4\pi e}{\epsilon} (n_+ - n_-), \quad (3)$$

where K_w and k_a denote the ion product and rate constant for ion association, respectively. In weak electrolytes, the ratio of dissociated to undissociated neutral compound is so small that the density of the neutral compound can be approximated as a constant. Using the dissociation rate constant k_d , $k_a K_w$ can be expressed as k_d multiplied by the concentration of undissociated compound, which also has a constant value. Therefore, we express the increasing rate of the ion concentration by dissociation using the ion product constant K_w . In the following, we consider steady states. The left-hand sides of Eqs. (1) and (2) are zero in steady states. The electrostatic potential difference relative to the electrostatic potential at L can be defined by

$$V(x) = - \int_x^L dx_1 E(x_1), \quad (4)$$

and can be calculated by solving Eqs. (1)–(3) under proper boundary conditions. The total potential difference between the electrode surface and bulk (overpotential) is $V(0)$.

A. Boundary Conditions for Ion Concentrations

At a sufficiently large distance away from the electrode surface, the ion concentrations are not affected by surface reactions. Correspondingly, we set boundary conditions at $x = L$ and assumed equal concentrations of cations and anions given by n_b . Boundary conditions at $x = L$ are given by

$$n_+|_{x=L} = n_b, \quad (5)$$

$$n_-|_{x=L} = n_b, \quad (6)$$

where n_b satisfies $K_w = n_b^2$.

We consider the case where cations are reduced at the interface between the electrolyte and electrode and the anions are reflected. Boundary conditions at the cathode located at $x = 0$ can be expressed as

$$D_+ \left(\frac{\partial n_+}{\partial x} - \frac{eEn_+}{k_B T} \right) \Big|_{x=0} = k_s [n_+ - n_s] \Big|_{x=0}, \quad (7)$$

$$D_- \left(\frac{\partial n_-}{\partial x} + \frac{eEn_-}{k_B T} \right) \Big|_{x=0} = 0. \quad (8)$$

The left-hand sides of Eqs. (7) and (8) represent the probability currents of cations and anions, respectively. Equation (8) indicates that anions are reflected by the cathode. In Eq. (7), the rate of forward reaction is proportional to the cation concentration expressed by n_+ at $x = 0$ (electrode surface) and that of the back reaction is expressed by $k_s n_s$,²⁴ where n_s is a phenomenological parameter introduced by Chang and Jaffé; n_s represents $n_+(0)$ at local equilibrium. The approach by Chang and Jaffé might be related to boundary conditions set by considering surface reaction rate equations. It has been shown that a reversible surface reaction described by the Langmuir adsorption-desorption process corresponds to the perfectly reflecting (blocking) boundary condition in the steady state.²⁵ For a certain irreversible surface reaction, the same boundary condition given by Chang and Jaffé can be derived in the steady state as shown in Appendix A. As a plausible boundary condition for irreversible surface reactions, we considered that $n_s = 0$ on the right-hand side of Eq. (7). The boundary condition is suitable to study the case when the overall reactions are limited by ion transport to the electrode surface. For partially reversible surface reactions, we set n_s being constant on the right-hand side of Eq. (7). The boundary condition is widely applicable including the case that the overall reactions are limited by surface reactions.

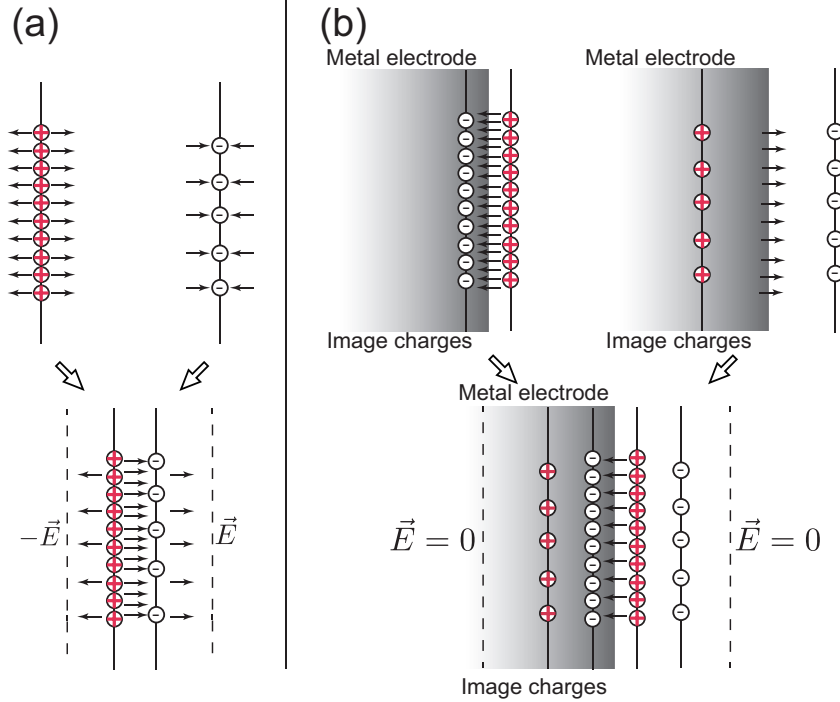


FIG. 2. (Color online) Boundary conditions for electric fields in one dimension (1D) were obtained by considering the superposition of electric fields from charges. Positive charges are indicated in red. (a) A system composed of electrolyte alone. The 1D fields from any charges are symmetric with respect to both positive and negative directions. The electric fields at the right and left dashed lines have the same strength and opposite direction. (b) A system composed of electrolyte and a metal electrode. The electric field at the dashed line is zero because the net charge inside the dashed lines is zero in the presence of image charges. Because the electric field at the right edge is zero, the electric field at the interface between the electrolyte and metal electrode can be calculated by assuming a 1D system. The resultant field strength at this interface is twice that in (a) when the left edge of the electrolyte is as indicated by the left dashed line in (a).

B. Boundary Conditions for Electric Fields

As the simplest situation, we first considered an isolated electrolyte, as shown in figure 2. Subsequently, we examined the effect of including metal (conducting) electrodes.

In 1D, the electric field from a charged plane is symmetric with respect to the positive

and negative directions. The electric field is obtained from Eq. (3) as

$$E(x) = \frac{2\pi e}{\epsilon} \left[\int_0^x dx_1 (n_+(x_1) - n_-(x_1)) - \int_x^L dx_1 (n_+(x_1) - n_-(x_1)) \right]. \quad (9)$$

The electric field at the interface between the electrode and electrolyte can be obtained from Eq. (9) as

$$E(0) = -\frac{2\pi e}{\epsilon} \int_0^L dx (n_+(x) - n_-(x)) \quad (10)$$

and the boundary condition is expressed by

$$E(0) = -E(L). \quad (11)$$

The electric fields at both boundaries denoted by the dashed lines in figure 2(a) should be symmetric for any charge distribution of a charged plane.

When a metal electrode is present, the boundary conditions for the electric fields are obtained using image charges inside the metal electrode, as illustrated in figure 2(b). The net image charge is the same as the net charge in the electrolyte system. Therefore, the electric fields at the boundaries enclosing both the real charges in the electrolyte and the image charges are zero. This situation can also be viewed from another perspective. Because we consider neutral products from a neutral electrolyte by electrode reactions, the net charge in the system including those induced in the electrode should be neutral. In this case, electric fields at some distance sufficiently far from the electrodes should be zero.⁶ The boundary condition is expressed as

$$E(L) = 0. \quad (12)$$

The electric field at the interface between an electrode and electrolyte can be obtained from Eq. (3) as

$$E(0) = \frac{4\pi}{\epsilon} \sigma^{(M)} \quad (13)$$

$$\sigma^{(M)} = -e \int_0^L dx [n_+(x) - n_-(x)]. \quad (14)$$

$\sigma^{(M)}$ indicates the electronic surface charge density on the metal and is given by integration of the image charge density in the metal: the amount of total image charges is equal to that of total real charges in the electrolytes and the image charges must have opposite sign of the

real charges.²⁶ Eq. (12) and Eq. (13) satisfy $E(L) - E(0) = 4\pi(e/\epsilon) \int_0^L dx [n_+(x) - n_-(x)]$ obtained by integrating Eq. (3). The electric field vectors at the interface between an electrode and electrolyte should be normal to the interface. However, at other locations, field lines in the presence of image charges are three-dimensional in nature.²⁷ In 1D PNP equations, 1D electric field lines are assumed. For poor conductors like semiconductor electrodes, if the electric fields inside a semiconductor could be zero because of the sufficient density of majority carriers, we chose the left dashed line in figure 2(b) sufficiently far away from the interface and obtained the same boundary condition given by Eq. (12). Below, we study the case where the boundary condition for an electrostatic potential is given by Eq. (12), for which the effect of electrode image charges is approximately taken into account.

C. Dimensionless Equations

We can express concentrations of cations and anions in dimensionless units as

$$N_+ = \frac{n_+}{n_b}, N_- = \frac{n_-}{n_b}, N_s = \frac{n_s}{n_b}. \quad (15)$$

For convenience, we introduce¹¹

$$\bar{D} = \frac{2D_+D_-}{D_+ + D_-}, \Delta = \frac{D_+ - D_-}{D_+ + D_-}. \quad (16)$$

Using the above definitions, the original diffusion constants can be obtained by $D_+ = \bar{D}/(1 - \Delta)$, and $D_- = \bar{D}/(1 + \Delta)$. By using the Debye length given by^{11,12,28-30}

$$\lambda_D = \left(\frac{\epsilon k_B T}{8\pi e^2 n_b} \right)^{1/2}, \quad (17)$$

we can express the characteristic electric field strength and diffusion time as¹¹

$$E_0 = \frac{k_B T}{e\lambda_D} = \left(\frac{8\pi n_b k_B T}{\epsilon} \right)^{1/2}, t_0 = \frac{\lambda_D^2}{\bar{D}} = \frac{\epsilon k_B T}{8\pi e^2 n_b \bar{D}}. \quad (18)$$

We also introduce dimensionless variables given by

$$y = \frac{x}{\lambda_D}, \tau = \frac{t}{t_0}, \xi = \frac{E}{E_0}. \quad (19)$$

Finally, we express the reaction rate constants in the dimensionless form,

$$\bar{k}_a = \frac{\lambda_D^2 k_a n_b}{\bar{D}}, \bar{k}_s = \frac{k_s \lambda_D}{D_+}. \quad (20)$$

Here, \bar{k}_a represents the dimensionless ion association rate constant and \bar{k}_s is the dimensionless surface reaction rate constant. Equation (1)–(3) can be rewritten using the dimensionless variables as

$$\frac{\partial^2 N_+}{\partial y^2} - \frac{\partial}{\partial y} (\xi N_+) = (1 - \Delta) \left[\frac{dN_+}{d\tau} - \bar{k}_a (1 - N_+ N_-) \right], \quad (21)$$

$$\frac{\partial^2 N_-}{\partial y^2} + \frac{\partial}{\partial y} (\xi N_-) = (1 + \Delta) \left[\frac{dN_-}{d\tau} - \bar{k}_a (1 - N_+ N_-) \right], \quad (22)$$

$$\frac{\partial}{\partial y} \xi = \frac{1}{2} (N_+ - N_-). \quad (23)$$

Similarly, boundary conditions at $y = L/\lambda_D$ are given by

$$N_+|_{y=L/\lambda_D} = 1, \quad (24)$$

$$N_-|_{y=L/\lambda_D} = 1, \quad (25)$$

and boundary conditions at $y = 0$ are given by

$$\left(\frac{\partial N_+}{\partial y} - \xi N_+ \right) \Big|_{y=0} = \bar{k}_s (N_+ - N_s) \Big|_{y=0}, \quad (26)$$

$$\left(\frac{\partial N_-}{\partial y} + \xi N_- \right) \Big|_{y=0} = 0. \quad (27)$$

Finally, the boundary condition for the electric field given by Eq. (12) can be expressed as

$$\xi|_{y=L/\lambda_D} = 0. \quad (28)$$

The potential difference given by Eq. (4) can be expressed as

$$V(y) = -E_0 \lambda_D \int_y^{y=L/\lambda_D} dy \xi(y). \quad (29)$$

III. ANALYTICAL RESULTS

A. Weak Electrolytes

Because we are interested in the deviations from equilibrium concentrations induced by surface reactions, we introduce sum and change as¹¹ $S = N_+ + N_-$, $C = N_+ - N_-$, where S and C characterize the mass density and charge density, respectively. To investigate the deviations from equilibrium states, we introduce

$$\delta S = S - 2, \delta C = C. \quad (30)$$

In steady states, Eqs. (21)–(23) can be rewritten using these variables as

$$\frac{\partial^2 \delta S}{\partial y^2} - \frac{\partial}{\partial y} (\xi \delta C) = -2\bar{k}_a \left[\delta S + \frac{1}{4} (\delta S^2 - \delta C^2) \right], \quad (31)$$

$$\frac{\partial^2 \delta C}{\partial y^2} - \frac{\partial}{\partial y} [\xi (\delta S + 2)] = 2\Delta\bar{k}_a \left[\delta S + \frac{1}{4} (\delta S^2 - \delta C^2) \right], \quad (32)$$

$$\frac{\partial}{\partial y} \xi = \frac{1}{2} \delta C. \quad (33)$$

In a weak electrolyte, the dissociation of a small amount of the solute can be represented by the right-hand sides of Eqs. (31) and (32).

The boundary conditions at $y = L/\lambda_D$ can be written as

$$\delta S|_{y=L/\lambda_D} = 0, \quad (34)$$

$$\delta C|_{y=L/\lambda_D} = 0. \quad (35)$$

The boundary conditions at $y = 0$ can be expressed as

$$\left(\frac{\partial \delta S}{\partial y} - \xi \delta C \right) \Big|_{y=0} = \bar{k}_s \left(\frac{\delta S + \delta C}{2} + 1 - N_s \right) \Big|_{y=0}, \quad (36)$$

$$\left(\frac{\partial \delta C}{\partial y} - \xi (\delta S + 2) \right) \Big|_{y=0} = \bar{k}_s \left(\frac{\delta S + \delta C}{2} + 1 - N_s \right) \Big|_{y=0}. \quad (37)$$

The boundary condition for the electric field is given by Eq. (28) when the effect of a conducting electrode is taken into account.

By linearizing the above equations, we solved the following set of equations,

$$\frac{\partial^2 \delta S}{\partial y^2} = -2\bar{k}_a \delta S, \quad (38)$$

$$\frac{\partial^2 \delta C}{\partial y^2} - 2\frac{\partial}{\partial y} \xi = 2\Delta\bar{k}_a \Delta \delta S. \quad (39)$$

By substituting Eq. (33) into Eq. (39), we obtain

$$\frac{\partial^2 \delta C}{\partial y^2} - \delta C = 2\Delta\bar{k}_a \Delta \delta S. \quad (40)$$

If the right-hand side is zero, Eq. (40) is equal to the equation derived by Debye and Falkenhagen in the steady state.³¹ The right-hand side of Eq. (40) reflects ionization of molecules. When the ion concentrations are conserved, the Debye Falkenhagen equation is obtained and the length scale of charge density variation is characterized by the Debye length. Equation (40) indicates that the charge density variation is still characterized by the Debye

length even when the ion concentrations are non-conserved by ionization of molecules: the ionization effect is represented by the inhomogeneous term in Eq. (40) when the linearization approximation is used. The validity of the linearization will be discussed later. Hereafter, we solve Eqs. (38), (40) and (33) using the boundary conditions given by Eqs. (34)-(37) and (28).

We obtained $\delta S(y) = 0$ from the boundary condition given by Eq. (34) in the limit of $L \rightarrow \infty$. Using the boundary condition given by Eq. (35) in the limit of $L \rightarrow \infty$, we obtained $\delta C(y) = C_c \exp(-y)$, where C_c is an integration constant. By substituting $\delta S(y) = 0$ into Eqs. (36) and (37) and linearizing the equations, the boundary conditions at $y = 0$ simplified to

$$\left. \frac{\delta C}{2} + 1 - N_s \right|_{y=0} = 0. \quad (41)$$

Using Eq. (41), we determined that the integration constant was $C_c = -2(1 - N_s)$. By substituting δC and integrating Eq. (33), we found that $\xi(y) = 2(1 - N_s) \exp(-y) + C_\xi$, where C_ξ is an integration constant. The boundary condition given by Eq. (28) can be expressed as $\xi(y) \rightarrow 0$ in the limit of $L \rightarrow \infty$. Therefore, we find that $C_\xi = 0$. These results can be written as

$$\delta C(y) = -2(1 - N_s) \exp(-y), \quad (42)$$

$$\xi(y) = (1 - N_s) \exp(-y). \quad (43)$$

The electric field strength can be written as

$$E(y) = \frac{k_B T}{e \lambda_D} (1 - N_s) \exp(-y). \quad (44)$$

From Eq. (29) and taking the limit of $L \rightarrow \infty$, the potential profile can be obtained as

$$V(y) = \frac{k_B T}{e} (1 - N_s) \exp(-y). \quad (45)$$

Using $N_+ = (2 + \delta C)/2$ and $N_- = (2 - \delta C)/2$, we obtained the ionic concentration profiles as

$$N_+(y) = 1 - (1 - N_s) \exp(-y), \quad (46)$$

$$N_-(y) = 1 + (1 - N_s) \exp(-y), \quad (47)$$

and the electrostatic potential profile can be expressed as

$$V(y) = \frac{k_B T}{e}(1 - N_+). \quad (48)$$

The dimensionless probability current density in Eq. (26) was obtained from Eqs. (46) and (43) as

$$\left(\frac{\partial N_+}{\partial y} - \xi N_+ \right) = (1 - N_s)^2 \exp(-2y). \quad (49)$$

The ion current density can be expressed as

$$e \frac{D_+}{\lambda_D} n_b \left(1 - \frac{n_s}{n_b} \right)^2 \exp(-2x/\lambda_D), \quad (50)$$

and its value at the electrode surface is given by

$$e \frac{D_+}{\lambda_D} n_b \left(1 - \frac{n_s}{n_b} \right)^2, \quad (51)$$

using a linearized approximation.

The above results were derived by linearizing the Poisson–Nernst–Planck equations with the association and dissociation reactions. The linearization is valid if $|\partial(\xi\delta C)/\partial y|$ on the left-hand side of Eq. (31) is smaller than $2\bar{k}_a|\delta S|$ on the right-hand side. The linearized solutions indicate $\delta C\partial\xi/\partial y = \xi\partial\delta C/\partial y$ and $|\partial(\xi\delta C)/\partial y| = 2\delta C\partial\xi/\partial y$. The charge density δC would decrease by increasing the distance from the electrode surface and $\delta C\partial\xi/\partial y = \delta C^2/2 \approx 2(1 - N_s)^2$ near the electrode surface. If the electrode is perfectly reactive, we have $\delta C\partial\xi/\partial y \approx 2$ and $|\partial(\xi\delta C)/\partial y| = 2\delta C\partial\xi/\partial y \approx 4$ near the electrode surface. By considering $\delta S \approx N_- \approx |\delta C|$, we also obtain $\delta S \approx 2$ near the electrode surface if the electrode is perfectly reactive. The condition for linearization given by $|\partial(\xi\delta C)/\partial y| \ll 2\bar{k}_a|\delta S|$ can be expressed as $1 \ll \bar{k}_a$. This condition corresponds to that of weak electrolytes. Otherwise, the coupling between ξ and δC in Eq. (31) cannot be ignored.

B. Strong Electrolytes

In strong electrolytes, ions are always dissociated. If we denote the concentrations of positively and negatively ionized monovalent ions as n^+ and n^- , respectively, the terms representing association and dissociation reactions on the right-hand sides of Eqs. (1) and (2) should be absent. As mentioned above, linearization fails for strong electrolytes, where

$\bar{k}_a \ll 1$. In the absence of association and dissociation reactions, approximate analytical solutions of the Poisson–Nernst–Planck equations have been studied more than decades. Here, we summarize some of the results.

As shown in Appendix B, the potential difference known as the diffusion potential is obtained,^{3,9–11}

$$V_{\text{HP}} = - \int_{x=0}^{x=L} dx E(x) = \frac{k_{\text{B}}T}{e} \frac{D_+ - D_-}{D_+ + D_-} \ln \left(\frac{n_s}{n_b} \right). \quad (52)$$

Equation (52) is also called the Henderson–Planck equation. The Nernst equation is reproduced by setting $D_+ = 0$, where the cation mass transport is absent and local equilibrium is maintained. In strong electrolytes, the potential difference is reduced from the Nernst equation by the factor given by $(D_+ - D_-)/(D_+ + D_-)$. The Henderson–Planck equation represents the diffusion potential caused by different diffusion constants of anions and cations.^{3,9–11}

In the asymptotic long time limit, the concentration profile is obtained from Eq. (B.20) using $\text{erf}(x) \sim 2x/\sqrt{\pi}$ for $x \ll 1$ as

$$N_+(y) = 1 + \delta S^{(0)}(y/\sqrt{\tau})/2 \sim \frac{n_s}{n_b} + \left(1 - \frac{n_s}{n_b} \right) \frac{y}{\sqrt{\pi\tau}}. \quad (53)$$

Similarly, the potential profile in the asymptotic limit is obtained from Eq. (B.25) as

$$V(y) \sim \frac{k_{\text{B}}T}{e} \frac{D_+ - D_-}{D_+ + D_-} \ln \left(\frac{n_s}{n_b} + \left(1 - \frac{n_s}{n_b} \right) \frac{y}{\sqrt{\pi\tau}} \right). \quad (54)$$

Equation (53) and (54) indicate that the concentration gradient and electrostatic potential profile become long-ranged as time proceeds. In other words, these are dynamical quantities.¹² According to Eq. (53), the concentration is a linear function of the distance from the electrode surface. Such linear distance dependence is in sharp contrast to the exponential distance dependence in Eq. (42) obtained for weak electrolytes. The potential profile is also long-ranged compared to the distance dependence in Eq. (45) obtained for weak electrolytes. The long-range nature of the concentration and potential profiles indicates that the steady-state profiles tend to depend on the system size defined by L because the spatial range of concentration gradient increases over time and exceeds the system size. In other words, the limit of $L \rightarrow \infty$ is singular in the sense that it is impossible to obtain solutions to satisfy the boundary conditions.^{7,12} We did not study the limit of $\bar{k}_a \rightarrow 0$ using numerical simulations. In the numerical calculations, we assumed the association rate constant was

a small value and numerically checked whether the results depended on the system size or not. We show that by decreasing the value of \bar{k}_a , the profiles become long-ranged and the potential drop tends to approach the value obtained using Eq. (52).

IV. NUMERICAL RESULTS

In a steady state without convection, we numerically solved Eqs. (21)–(28) by the relaxation method. We present the numerical results obtained using the boundary condition including the effect of the electrode. The concentration profiles were almost the same if we used the boundary condition for an isolated electrolyte without taking into account the effect of the electrode.

As a concrete example, we study electrochemical reduction of water at electrode surfaces yielding hydrogen. Water is a weak electrolyte and the dissociation of a small amount of water can be represented by the association and dissociation reaction terms in Eqs. (31) and (32). The diffusion constants of H_3O^+ and OH^- are $9.4 \times 10^{-9} \text{ m}^2/\text{s}$ and $5.3 \times 10^{-9} \text{ m}^2/\text{s}$, respectively.³² By substituting $D_+ = 9.4 \times 10^{-9} \text{ m}^2/\text{s}$ and $D_- = 5.3 \times 10^{-9} \text{ m}^2/\text{s}$ into Eq. (16), we obtained $\bar{D} = 6.78 \times 10^{-9} \text{ m}^2/\text{s}$ and $\Delta = 0.28$. Using $n_b = 1 \times 10^{-7} \text{ mol/L}$, the Debye length was obtained as $\lambda_D = 9.8 \times 10^{-7} \sim 10^{-6} \text{ m}$.

A. Comparison of Weak and Strong Electrolytes

In figure 3, we compare the results of the Nernst equation, the Henderson–Planck equation, and Eq. (48). The electrostatic potential profile of the Nernst equation can be expressed as

$$V_N(x) = \frac{k_B T}{e} \ln \frac{n_b}{n_+(x)}, \quad (55)$$

which is equivalent to the local equilibrium assumption given by

$$\frac{n_+(x)}{n_b} = \exp \left[-\frac{eV_N(x)}{k_B T} \right], \quad (56)$$

where ion mass flows are assumed to be absent. The Nernst equation is irrelevant for strong electrolytes because electrode reactions induce ion mass flows in particular in the absence of ionization and association of ions. The Nernst equation may be applicable in weak

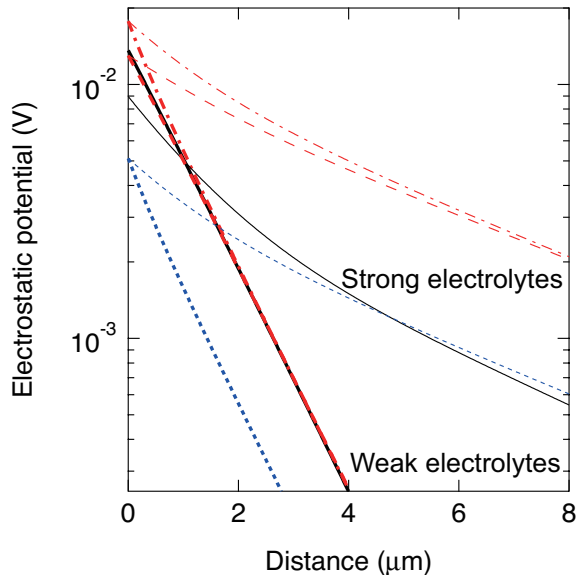


FIG. 3. (Color online) Electrostatic potential as a function of distance from the electrode when $N_s = 0.5$. Thick lines indicate $\bar{k}_a = 2.0$ (weak electrolytes) and thin lines indicate $\bar{k}_a = 0.02$ (strong electrolytes). The solid lines represent the numerical solutions. (Red) dash-dotted lines represent the results of the Nernst equation given by Eq. (55). (Red) long dashed lines represent the results of Eq. (48). (Blue) short dashed lines represent the results of the Henderson–Planck equation given by Eq. (57).

electrolytes when $\bar{k}_a \gg 1$, where the rate of ion dissociation and association given by $k_a n_b$ is much higher than the inverse of the time required to diffuse over the Debye length given by \bar{D}/λ_D^2 . The electrostatic potential profile of the Henderson–Planck equation is given by

$$V_{\text{HP}}(x) = \frac{k_B T}{e} \frac{D_+ - D_-}{D_+ + D_-} \ln \left(\frac{n_+(x)}{n_b} \right), \quad (57)$$

which is obtained for strong electrolytes.

The conditions $\bar{k}_a = 2.0$ and $\bar{k}_a = 0.02$ correspond to weak and strong electrolytes, respectively. When $\bar{k}_a = 2.0$, the result of the Nernst equation is closer to the numerical result than that of the Henderson–Planck equation. However, the result of the Nernst equation deviates from the numerical result near the electrode. The potential profile obtained from Eq. (48) is close to the numerical result for all distances. Equation (48) was obtained by linearization of full transport equations and the Poisson equation. This result is valid for weak electrolytes. The Nernst equation was obtained by assuming local equilibrium, where mass currents were not taken into account. The deviation found near the electrode could be

caused by mass currents. When charge neutrality is broken near the electrode surface, both ionization and ion transport occur to recover charge neutrality. Because of ion transport, the local equilibrium assumption used to obtain the Nernst equation is violated, particularly near the electrode surface. The Henderson–Planck equation is derived for strong electrolytes and its results cannot be applied to weak electrolytes.

For strong electrolytes indicated by $\bar{k}_a = 0.02$, the result of the Henderson–Planck equation is closer to the numerical result than that of the Nernst equation. The Henderson–Planck equation is derived for strong electrolytes, where ionization is not taken into account. In strong electrolytes, most molecules are ionized and the effect of ionization of a small amount of unionized molecules can be ignored. In contrast, the Nernst equation is derived by assuming local equilibrium, which can be violated by ionic currents. We should note that breakdown of charge neutrality can be recovered only by mass currents in strong electrolytes, whereas it can also be recovered by ionization in weak electrolytes. Correspondingly, larger deviations from the exact results are found in strong electrolytes compared with the case for weak electrolytes if electrostatic potentials are estimated by the Nernst equation. It should be noted that Eq. (48) was derived by assuming weak electrolytes and that its results are not valid for strong electrolytes.

In figure 4, we show concentrations of cations and anions as a function of distance from the electrode surface in strong and weak electrolytes. In weak electrolytes, both cation and anion concentrations deviate from the bulk concentration when the distance from the electrode is within a few Debye lengths. Concentration profiles of cations are long-ranged in strong electrolytes. Interestingly, the cation and anion concentrations were different when the distance from the electrode was within a few Debye lengths in both strong and weak electrolytes. In other words, charge density caused by breakdown of charge neutrality was observed approximately within the surface layer to a depth of a few Debye lengths. The anion concentration profile is similar to that of cations outside this layer in strong electrolytes due to charge neutrality. The difference between the spatial range of charge density and that of mass density for strong electrolytes has been pointed out.⁴ Although small, the increase of anion concentration near the electrode surface seen in figure 4 could be caused by ionization of a small amount of unionized molecules present in the strong electrolyte characterized by $\bar{k}_a = 0.02$.

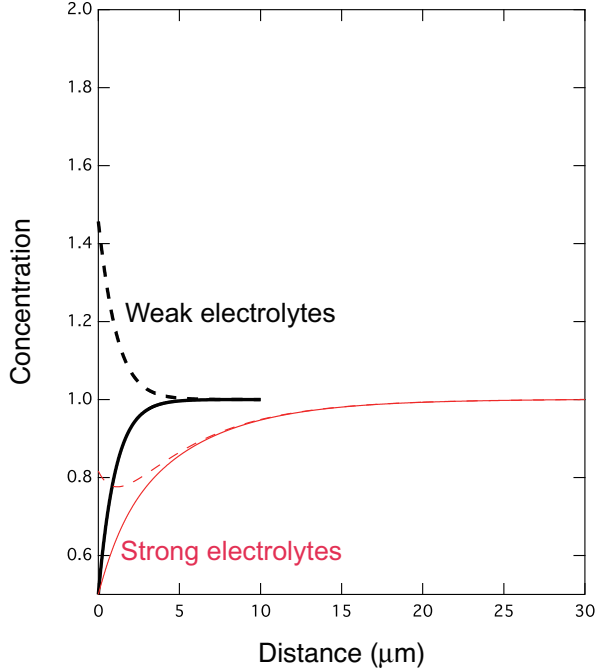


FIG. 4. (Color online) Concentrations of cations and anions as a function of distance from the electrode when $N_s = 0.5$. Thick black lines indicate $\bar{k}_a = 2.0$ (weak electrolytes) and thin (red) lines indicate $\bar{k}_a = 0.02$ (strong electrolytes). The solid lines represent cation concentrations and dashed lines represent anion concentrations.

B. Precise Results for Weak Electrolytes

Here, we consider water as a weak electrolyte and study ion concentrations, ion currents, and electrostatic potentials in weak electrolytes to assess the linearized solutions. The maximum error of linearization can be found by imposing the perfectly absorbing boundary condition where the surface concentration is zero because of fast surface reaction. We study the results obtained under the perfectly absorbing boundary condition.

The dissociation and association rate constants of water are $k_a = 1.4 \times 10^{11} \text{L}/(\text{mol s})$ and $k_d = 2.5 \times 10^{-5} \text{1/s}$, respectively.³³ We obtained $k_a n_b = 1.4 \times 10^4 \text{1/s}$ using $n_b = 1 \times 10^{-7} \text{mol/L}$. By substituting these values into Eq. (20), i.e., $\bar{k}_a = \lambda_D^2 k_a n_b / \bar{D}$, we find that $\bar{k}_a = 2$. The value of $1/(k_a n_b)$ gives a time scale of $0.7 \times 10^{-4} \text{s}$. The time scale of diffusion over the Debye length was estimated as $t_0 = \lambda_D^2 / \bar{D} = 1.5 \times 10^{-4} \text{1/s}$. These values indeed indicate that the time scale of association and dissociation reactions is comparable to that of diffusion over the Debye length. Therefore, charge neutrality could be recovered

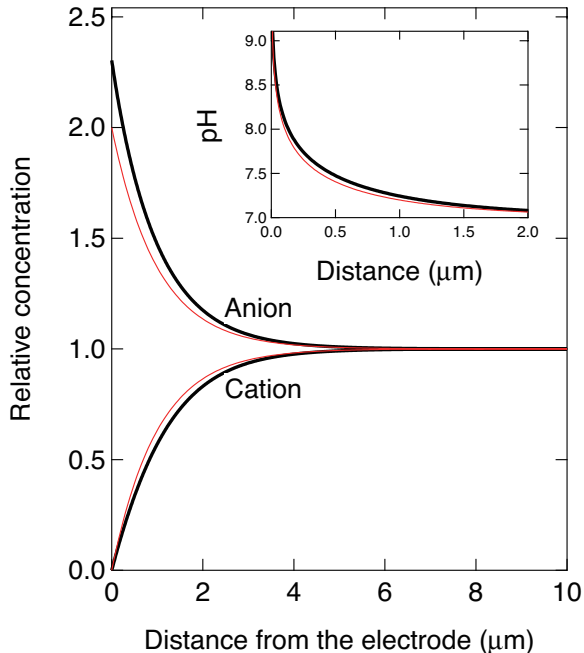


FIG. 5. (Color online) Concentrations of cations and anions as a function of distance from the electrode for the perfectly absorbing boundary condition, $k_s \rightarrow \infty$ and $n_s = 0$. The inset shows pH as a function of distance from the electrode. Thick black lines represent the exact numerical results. Thin (red) lines indicate the approximate results obtained using Eq. (46) for cations and Eq. (47) for anions.

by both ionization and ion currents in weak electrolytes.

Figure 5 displays the concentration profiles produced when the perfectly absorbing boundary condition was imposed. The cation concentration profile and the pH obtained using Eq. (46) are close to the exact numerical results. The anion concentration profile obtained using Eq. (47) is slightly lower than the numerical results. However, the deviation is at most 12%.

The electric field obtained using Eq. (44) and electrostatic potential obtained using Eq. (45) are again slightly smaller than the exact numerical results, as shown in figure 6. The electrostatic potential at the surface is approximately 0.03 V different from the bulk value. Thus, the electrostatic potential difference for a monovalent ion is on the same scale as thermal energy at room temperature. Therefore, this difference is reasonable as a thermally generated internal potential.

In figure 7, we compare the results of Eq. (48) with those of the Nernst equation given by Eq. (55). The results of both Eq. (48) and the Nernst equation were obtained using the

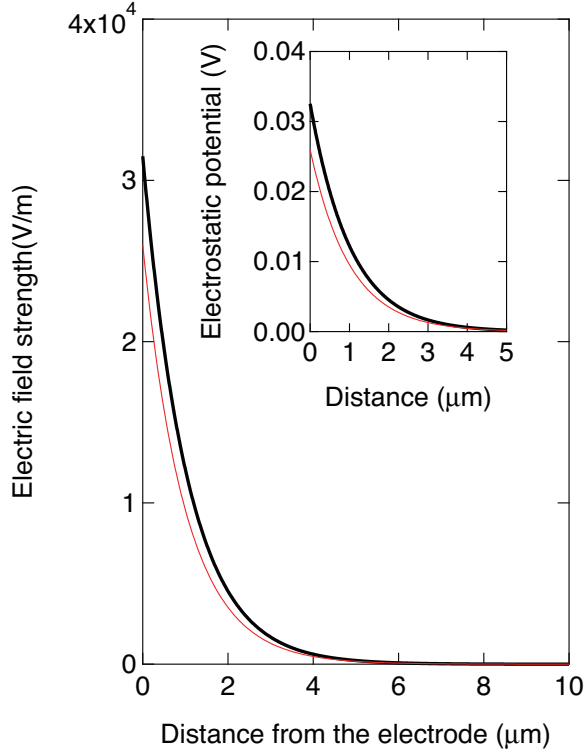


FIG. 6. (Color online) Electric fields as a function of distance from the electrode for the perfectly absorbing boundary condition, $k_s \rightarrow \infty$ and $n_s = 0$. The inset shows electrostatic potentials as a function of distance from the electrode. Thick black lines depict exact numerical results. The thin (red) line indicates the result of Eq. (44) for electric field strength and Eq. (45) for electrostatic potential.

numerical values of ion concentrations as inputs. Noting the scale change in the abscissa between figures 6 and 7, we see that the deviations between the numerical results and those of Eq. (45) are decreased by substituting the numerically obtained values of N_+ in Eq. (48). We can also see that the linearized solution is closer to the numerical result than the result of the Nernst equation. The same conclusion can be drawn from figure 3, where the surface concentration is given by $N_s = 0.5$. According to the approximate solution given by Eq. (45), the electrostatic potential decreases exponentially with increasing distance from the electrode surface. This trend is confirmed in the inset of figure 7. Comparing figure 7 and 3 reveals that the deviations of linearized results from the exact results increase as the surface concentration decreases. When the surface concentration is low, the results of Eq. (48) are lower than the numerical results by at most 15% when the distance from the electrode is

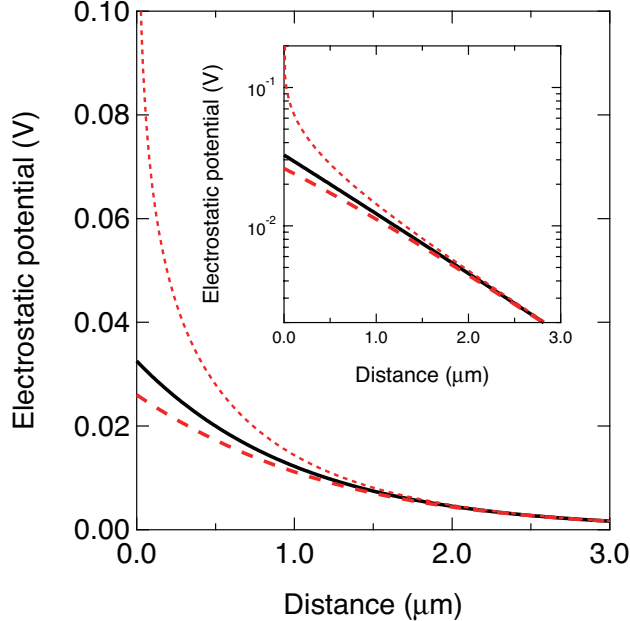


FIG. 7. (Color online) Electrostatic potential as a function of distance from the electrode when $N_s = 0$. The inset shows a semi-log plot. The thick black line indicates the exact numerical results. (Red) long dashed lines show the results of Eq. (48) using the numerical results for cation concentration. (Red) short dashed lines indicate the results of the Nernst equation given by Eq. (55).

less than a Debye length.

V. DISCUSSION

As shown in figure 7, electrostatic potential profiles deviated from those obtained from the Nernst equation as distance from the electrode surface decreased. By taking into account ion mass flows and ionization of weak electrolytes, we obtained an approximate expression for the electrostatic profiles given by,

$$V(x) = \frac{k_B T}{e} \left(1 - \frac{n_+(x)}{n_b} \right). \quad (58)$$

As shown in figure 7, Eq. (58) is more accurate than the Nernst equation near the electrode surface. That is, ion mass flows induced deviations of ion concentrations from the local equilibrium distributions assumed to obtain the Nernst equation. We obtained an approximate

expression for ion concentration profiles given by,

$$\frac{n_+(x)}{n_b} = 1 - \left(1 - \frac{n_s}{n_b}\right) \exp\left(-\frac{x}{\lambda_D}\right). \quad (59)$$

In terms of pH, the result can be expressed as

$$\text{pH}(x) = 7 - \log_{10} \left[1 - \left(1 - \frac{n_s}{n_b}\right) \exp\left(-\frac{x}{\lambda_D}\right) \right]. \quad (60)$$

As illustrated in figure 5, Eq. (59) approximately reproduces the numerical results. By rewriting Eq. (59), an approximate expression for potential profiles can be obtained as

$$V(x) = \frac{k_B T}{e} \left(1 - \frac{n_s}{n_b}\right) \exp\left(-\frac{x}{\lambda_D}\right), \quad (61)$$

and the potential difference between the bulk electrolyte and that at the electrode surface can be expressed as

$$V(0) = \frac{k_B T}{e} \left(1 - \frac{n_s}{n_b}\right). \quad (62)$$

These results indicate the importance of ion mass flows to obtain the correct ion profiles and electrostatic potentials in weak electrolytes.

Exponential screening of Eq. (61) reminds us of the exponential decrease of electric field formed near charged surfaces in strong electrolytes under local equilibrium^{12,28–30,34}, the solution for a certain boundary condition is known as the Debye–Hückel theory. However, the situation considered here is different from that of the Debye–Hückel theory. The Debye–Hückel theory is based on the Poisson–Boltzmann equation, where ion concentrations are assumed to obey local equilibrium. Here, we solved the e-PNP equations where the effect of ion currents is taken into account and deviations from the local equilibrium distributions can be studied.

For water, the ion current of cations at the electrode surface can be estimated using the Debye length and bulk concentration denoted by n_b using Eq. (51). The concentration gradient can be approximately given by n_b/λ_D . By using $D_+ \approx 10^{-4}$ cm²/s, $\lambda_D \approx 10^{-4}$ cm, the ion current density can be expressed as

$$eD_+ \frac{n_b}{\lambda_D} \times 10^5 \text{ A/cm}^2 = 0.01 \text{ mA/cm}^2, \quad (63)$$

when the boundary condition is given by $n_+(0) = 0$ corresponding to the case where the back reaction can be ignored because of fast forward reactions at the interface, where 96500

C/mol is approximated by 10^5 C/mol. The above result matches with that of linearization given by Eq. (51) and is 30% smaller than the exact numerical result. To realize 10% PEC conversion efficiency under 1 sun, a current density of 10 mA cm^{-2} is required. The current obtained without convection caused by external sources at neutral pH is an order of magnitude smaller than this. This result indicates that ion currents may limit the overall efficiency because of the small diffusion constant of H_3O^+ compared with that of electrons. Convective flows can be forced by an external source but the forced convection consumes energy. However, convective flows can be also generated by the movement of evolving gas bubbles without an external source. For splitting of pure water, recent experimental setups have used internal convection caused by placing cathodic and anodic electrodes in parallel configurations.^{22,23} In this configuration, an extra energy source to generate convection was not needed. In principle, convective flows can be taken into account by introducing the hydrodynamic equation into the Nernst–Planck equations.³⁵ An extension of the present work to include convective flows will be important to study the case when current density is high.

VI. CONCLUSION

In a weak electrolyte, only a small fraction of the solute dissociates into ions. We considered the case where one of the ion species reacted at the electrode surface, so charge neutrality was broken at the electrode surface. Breakdown of charge neutrality resulted in charge accumulation near the electrode surface. Correspondingly, an electrostatic potential gradient was generated. In strong electrolytes, the effect of break-down of charge neutrality on ion mass density profiles has been known to be limited only near the electrode surface whereas the mass density variation can be long-ranged.^{1-4,12} Here, by taking into account ion mass flows in weak electrolytes, we obtained analytical expressions for the electrostatic potential at the electrode surface relative to that in the bulk (overpotential) [Eq. (58)] and ionic currents at the electrode surface [Eq. (51)] as well as density profiles [Eq. (59)] and electrostatic potential gradients [Eq. (61)]. The validity of these solutions was checked by comparison to the numerical solutions.

Both the charge density (difference between cation and anion concentrations for a monovalent electrolyte) gradient and ion mass density profiles were characterized by the Debye

length in weak electrolytes. We showed that exponential screening occurs for the charge density, ion mass density, and electrostatic potential profiles in weak electrolytes under ionic current flows. In strong electrolytes, although the charge density gradient was still characterized by the Debye length, ion mass density profiles were long-ranged compared to exponential screening with the Debye length.⁴

In strong electrolytes, a large fraction of molecules are ionized and charge neutrality is essentially recovered by mass transport. For a strong electrolyte, the overpotential can be obtained from the Henderson–Planck equation given by Eq. (52). Conversely, in weak electrolytes, the Henderson–Planck equation does not hold because charge neutrality can be recovered by ionization of molecules. When charge neutrality is broken in a weak electrolyte, neutrality can be recovered by both mass transport and ionization. Our results show that both processes compete and should be taken into account simultaneously. In 1:1 monovalent weak electrolytes, ion mass density profiles as well as charge density variation were short-ranged and the length scale was characterized by the Debye length. The analytical solutions take into account the competing between mass transport and ionization and are useful to estimate the electrostatic potential profiles and current densities in certain weak electrolytes.

The results of this paper are related to photoelectrochemical (PEC) water splitting. Although theoretically estimated PEC conversion efficiency exceeds 10%,^{36–41} such high efficiency has not yet been achieved without an external energy supply.^{36,42,43} Unlike photovoltaics, the PEC conversion efficiency can be limited by electrochemical processes occurring at the interface between an electrode and electrolyte even if a semiconductor with a suitable band gap is used. There could be two main limiting factors for PEC conversion efficiency related to the electrode–electrolyte interface.

The first limitation of PEC conversion efficiency could be that ion mobilities can be lower than electron mobilities in semiconductors. As explained in the previous section, steep ion concentration gradients would be preferable to induce ion currents to resolve the inhomogeneous ion distribution. We have shown that the concentration gradients are characterized by the Debye length for 1:1 monovalent weak electrolytes. However, the Debye length is smaller than the spatial resolution of measurements using pH indicator dyes.²⁰ For water-splitting reactions, multi-ionic solutions are commonly used to control electrostatic potentials and/or engineer the pH of electrolytes.^{19,20,44} Observed large scale pH gradients could result from multiple ionic species. Indeed, 1:1 weak electrolyte is special, in which both charge den-

sity gradients and ion concentration gradients are characterized by the single length scale through the ion product constant; deviation of a local cation concentration from the bulk concentration should accompany with deviation of a local anion concentration because the product of both concentrations is a constant. The length-scale separation between charge density profiles and concentration profiles could be possible for multi-ionic solutions.

The second limitation could be overpotential related to a charge density gradient near the electrode. Our results indicate that the overpotential is only on the same scale as thermal energy at room temperature. The overpotential is caused by a charge density gradient whose spatial extent is characterized by the Debye length. It should be noted that the charge density gradient can be estimated from the pH gradient only for pure water. In general, charge density cannot be estimated from pH alone in the presence of other ion species.

For simplicity, we considered the case that molecules can be ionized to monovalent ions in the absence of buffer electrolytes composed of weak acid and/or weak base. We also did not consider supporting electrolytes to increase conductivity of the bulk solution. The effect of multiple ionic species on ion currents could be taken into account using new numerical methods developed to calculate junction potentials,^{10,45} where the charge neutrality condition is unnecessary. The analytical method used in this paper should be extended to multi-ionic solutions in the future.

ACKNOWLEDGMENTS

This work was supported by the “Research Project for Future Development: Artificial Photosynthetic Chemical Process (ARPCChem)” (METI/NEDO, Japan: 2012-2022).

APPENDIX A. DERIVATION OF EQ. (7) FOR A CERTAIN SURFACE REACTION

If only linear reactions are considered as elementary reaction steps, n_s in Eq. (7) is a constant. Otherwise, n_s may depend on n_+ , as will be explained below. For this reason, we write $n_s(n_+)$ for n_s in this Appendix.

We consider the case where cations are reduced at the interface between the electrolyte and electrode and the anions are reflected. As an example, we consider the water splitting reaction expressed by



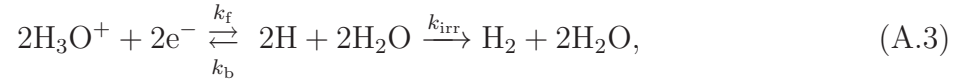
and the following half reaction at the cathode, i.e., the hydrogen evolution reaction (HER),



where we take into account the back reaction for generality.

The boundary conditions are related to the stoichiometry of elementary reactions. Precise elementary steps depend on semiconductor materials and are not completely understood.^{46–50} Here, we take into account two types of intermediate reaction steps in the HER.

If we consider reactions with an intermediate (the Volmer–Tafel mechanism) given by^{50–53}



the change rate of $n_+(0) = [\text{H}_3\text{O}^+](0)$ can be expressed as

$$k_f[e^-] \left(n_+(0) - \frac{k_b}{k_f[e^-]}[\text{H}] \right), \quad (\text{A.4})$$

where $[e^-]$ and $[\text{H}]$ represent the concentration of electrons and H at the electrode surface, respectively. Because other sources and sinks for n_+ are absent, this rate must be equal to the flux given by the left-hand side of Eq. (7). By comparing the right-hand side of Eq. (7) with Eq. (A.4), we find $k_s = k_f[e^-]$ and $n_s = k_b[\text{H}]/(k_f[e^-])$. When $k_b[\text{H}]/(k_f[e^-]) \ll [\text{H}_3\text{O}^+](0)$ is satisfied by using a suitable semiconductor to generate electrons, $n_s = 0$ can be assumed. In steady states, the gas production rate is given by⁵⁴

$$2k_{\text{irr}}[\text{H}]^2 = (k_f[e^-][\text{H}_3\text{O}^+] - k_b[\text{H}])\Big|_{x=0}. \quad (\text{A.5})$$

By comparing Eq. (A.5) with Eq. (A.4) and (7), the steady-state gas production rate can be expressed as

$$2k_{\text{irr}}[\text{H}]^2 = D_+ \left(\frac{\partial n_+}{\partial x} - \frac{eEn_+}{k_{\text{B}}T} \right) \Big|_{x=0}. \quad (\text{A.6})$$

For the HER with relatively simple reactions via an intermediate expressed by Eq. (A.3), the steady-state gas production rate is obtained from the probability current of cations at the electrolyte–electrode interface. In steady states, the concentration of the reaction intermediate ($[\text{H}]$) obeys the relation

$$k_{\text{f}}[\text{e}^-][\text{H}_3\text{O}^+](0) - k_{\text{b}}[\text{H}] - 2k_{\text{irr}}[\text{H}]^2 = 0 \quad (\text{A.7})$$

and the solution is obtained as

$$[\text{H}] = \frac{-k_{\text{b}} + \sqrt{k_{\text{b}}^2 + 8k_{\text{irr}}k_{\text{f}}[\text{e}^-]n_+(0)}}{4k_{\text{irr}}} \quad (\text{A.8})$$

$$\approx \frac{\sqrt{k_{\text{f}}[\text{e}^-]n_+(0)}}{\sqrt{2k_{\text{irr}}}} \text{ for } k_{\text{b}} \ll 2\sqrt{2k_{\text{irr}}k_{\text{f}}[\text{e}^-]n_+(0)}, \quad (\text{A.9})$$

where $n_+(0) = [\text{H}_3\text{O}^+](0)$ is used. By substituting Eq. (A.9) into Eq. (A.4), the right-hand side of Eq. (7) can be expressed as

$$k_{\text{f}}[\text{e}^-] \left(n_+(0) - \frac{k_{\text{b}}}{\sqrt{2k_{\text{irr}}k_{\text{f}}[\text{e}^-]}} \sqrt{n_+(0)} \right) \quad (\text{A.10})$$

and we find $n_{\text{s}}(n_+(0)) = k_{\text{b}}\sqrt{n_+(0)}/\sqrt{2k_{\text{irr}}k_{\text{f}}[\text{e}^-]}$. When the HER rate is fast and the condition $k_{\text{b}}\sqrt{n_+(0)}/(2\sqrt{2k_{\text{irr}}k_{\text{f}}[\text{e}^-]}) \ll 1$ is satisfied, the right-hand side of Eq. (7) can be approximated by $k_{\text{s}}n_+(0)$.

As a plausible reaction step, an intermediate step (the Volmer–Heyrovsky mechanism) given by $\text{H}_3\text{O}^+ + \text{e}^- + \text{H} \xrightarrow{k_{\text{irr}1}} \text{H}_2 + \text{H}_2\text{O}$ was also proposed instead of the second step in Eq. (A.3).^{48–53} From the reaction $\text{H}_3\text{O}^+ + \text{e}^- \xrightleftharpoons[k_{\text{b}}]{k_{\text{f}}} \text{H} + \text{H}_2\text{O}$ and the intermediate step, the change rate of $n_+(0)$ is obtained as

$$k_{\text{f}}[\text{e}^-] \left[\left(1 - \frac{k_{\text{irr}1}[\text{H}]}{k_{\text{f}}} \right) n_+(0) - \frac{k_{\text{b}}}{k_{\text{f}}[\text{e}^-]}[\text{H}] \right]. \quad (\text{A.11})$$

This rate must be equal to the flux given by the left-hand side of Eq. (7). The concentration of the reaction intermediate obeys the relation

$$k_{\text{f}}[\text{e}^-]n_+(0) - k_{\text{b}}[\text{H}] - k_{\text{irr}1}[\text{e}^-]n_+(0)[\text{H}] = 0, \quad (\text{A.12})$$

and the solution is obtained as

$$[\text{H}] = \frac{k_f[\text{e}^-]n_+(0)}{k_b + k_{\text{irr1}}[\text{e}^-]n_+(0)}. \quad (\text{A.13})$$

The right-hand side of Eq. (7) given by Eq. (A.11) can be expressed by

$$k_f[\text{e}^-] \left(1 + \frac{k_{\text{irr1}}[\text{e}^-]n_+(0)}{k_b + k_{\text{irr1}}[\text{e}^-]n_+(0)} \right) n_+(0) - \frac{k_b k_f[\text{e}^-]n_+(0)}{k_b + k_{\text{irr1}}[\text{e}^-]n_+(0)}. \quad (\text{A.14})$$

The above result indicates that boundary conditions have a non-linear dependence on $n_+(0)$ in place of $k_s n_+(0)$. When the gas production rate is faster than the back reaction, $k_b \ll k_{\text{irr1}}[\text{e}^-]n_+(0)$ is satisfied. In this case, the non-linear boundary condition can be linearized.

The right-hand side of Eq. (7) can be expressed as

$$\left[k_f[\text{e}^-]n_+ \left(1 + \frac{k_{\text{irr1}}[\text{e}^-]n_+}{k_b + k_{\text{irr1}}[\text{e}^-]n_+} \right) - \frac{k_b k_f[\text{e}^-]n_+}{k_b + k_{\text{irr1}}[\text{e}^-]n_+} \right] \Big|_{x=0} \quad (\text{A.15})$$

$$\approx 2k_f[\text{e}^-] \left(n_+ - \frac{k_b}{2k_{\text{irr1}}[\text{e}^-]} \right) \Big|_{x=0}, \quad (\text{A.16})$$

and we find that $n_s(n_+(0))$ is a constant given by $n_s(n_+(0)) = k_b / (2k_{\text{irr1}}[\text{e}^-])$.

APPENDIX B. DERIVATION OF EQ. (52)

We performed a systematic expansion in $1/\tau$ when $\bar{k}_a = 0$ by applying the approach developed to calculate liquid junction potential to our problem of surface reactions.¹¹ When concentration change is restored only by diffusion, a relevant variable is $z = y/\sqrt{\tau}$. In terms of the new variable, Eq. (21)–(23) can be rewritten using $\delta S = N_+ + N_- - 2$, $\delta C = N_+ - N_-$, and z by applying the chain rule for partials as

$$\frac{1}{\tau} \frac{\partial^2 \delta S}{\partial z^2} - \frac{\partial}{\partial z} \left(\frac{\xi}{\sqrt{\tau}} \delta C \right) = \frac{\partial}{\partial \tau} (\delta S - \Delta \delta C) - \frac{z}{2\tau} \frac{\partial}{\partial z} (\delta S - \Delta \delta C), \quad (\text{B.1})$$

$$\frac{1}{\tau} \frac{\partial^2 \delta C}{\partial z^2} - \frac{\partial}{\partial z} \left[\frac{\xi}{\sqrt{\tau}} (\delta S + 2) \right] = \frac{\partial}{\partial \tau} (\delta C - \Delta \delta S) - \frac{z}{2\tau} \frac{\partial}{\partial z} (\delta C - \Delta \delta S), \quad (\text{B.2})$$

$$\frac{\partial}{\partial z} \frac{\xi}{\sqrt{\tau}} = \frac{1}{2} \delta C. \quad (\text{B.3})$$

The diffusion may give rise to algebraic τ dependence,

$$\delta S(z, \tau) = \delta S(z)^{(0)} + \delta S(z)^{(1)}/\tau + \delta S(z)^{(2)}/\tau^2 + \dots, \quad (\text{B.4})$$

$$\delta C(z, \tau) = \delta C(z)^{(0)} + \delta C(z)^{(1)}/\tau + \delta C(z)^{(2)}/\tau^2 + \dots, \quad (\text{B.5})$$

$$\frac{\xi(z, \tau)}{\sqrt{\tau}} = \frac{\eta^{(1)}(z)}{\tau} + \frac{\eta^{(2)}(z)}{\tau^2} + \dots. \quad (\text{B.6})$$

$\eta^{(0)}(z)$ should be zero; otherwise, $\xi(z) \sim \sqrt{\tau} \eta^{(0)}(z)$ diverges as $\tau \rightarrow \infty$.

Now, we study the lowest-order solution given by the order of $1/\tau^0$. From Eq. (B.3), the charge neutrality condition is satisfied; i.e.,

$$\delta C(z)^{(0)} = 0. \quad (\text{B.7})$$

By substituting Eqs. (B.4) and (B.5) into Eqs. (B.1)–(B.3), we obtained $S^{(0)}(z)$ and $\eta^{(1)}(z)$ of the order of $1/\tau$ as

$$\frac{\partial^2 \delta S^{(0)}}{\partial z^2} = -\frac{z}{2} \frac{\partial}{\partial z} (\delta S^{(0)}), \quad (\text{B.8})$$

$$-\frac{\partial}{\partial z} [\eta^{(1)}(z)(\delta S^{(0)} + 2)] = \Delta \frac{z}{2} \frac{\partial}{\partial z} \delta S^{(0)}. \quad (\text{B.9})$$

Boundary conditions at $z = L/(\lambda_D \sqrt{\tau})$ are given by

$$\delta S^{(0)} \Big|_{z=L/(\lambda_D \sqrt{\tau})} = 0, \quad (\text{B.10})$$

$$\delta C^{(0)} \Big|_{z=L/(\lambda_D \sqrt{\tau})} = 0. \quad (\text{B.11})$$

Boundary conditions at $y = 0$ are expressed as

$$\frac{1}{\sqrt{\tau}} \frac{\partial \delta S^{(0)}}{\partial z} \Big|_{z=0} = \bar{k}_s \left(\frac{\delta S^{(0)}}{2} + 1 - N_s \right) \Big|_{z=0}, \quad (\text{B.12})$$

$$-\frac{1}{\sqrt{\tau}} \eta^{(1)}(\delta S^{(0)} + 2) \Big|_{z=0} = \bar{k}_s \left(\frac{\delta S^{(0)}}{2} + 1 - N_s \right) \Big|_{z=0}. \quad (\text{B.13})$$

In the limit of $\tau \rightarrow \infty$, the left-hand sides of Eqs. (B.12) and (B.13) should be zero; i.e.,

$$\delta S^{(0)} \Big|_{z=0} \approx 2(N_s - 1). \quad (\text{B.14})$$

The potential difference can be obtained from

$$V(z) = -E_0 \lambda_D \int_z^\infty dz_1 \eta^{(1)}(z_1), \quad (\text{B.15})$$

and the total potential difference between the electrode surface and bulk is $V = V(0)$.

First, we integrated Eq. (B.8) and obtained

$$\frac{\partial}{\partial z} (\delta S^{(0)}) = A_1 \exp\left(-\frac{z^2}{4}\right), \quad (\text{B.16})$$

where A_1 is an integration constant. By integrating the above equation, we have

$$\delta S^{(0)}(z) = A_0 + A_1 \int_0^z dz_1 \exp\left(-\frac{z_1^2}{4}\right), \quad (\text{B.17})$$

where A_0 is an integration constant.

We note that $\int_0^\infty dz_1 \exp\left(-\frac{z_1^2}{4}\right) = \sqrt{\pi}$. Using the boundary conditions given by Eqs. (B.10) and (B.12), we obtained

$$A_0 = 2(N_s - 1), \quad (\text{B.18})$$

$$A_1 = 2(1 - N_s)/\sqrt{\pi}. \quad (\text{B.19})$$

By substituting these equations into Eq. (B.17), it became

$$\delta S^{(0)}(z) = 2(1 - N_s)[-1 + \text{erf}(z/2)], \quad (\text{B.20})$$

where we used $\text{erf}(z/2) = (1/\sqrt{\pi}) \int_0^z dz_1 \exp(-z_1^2/4)$.⁵⁵ Note that $\lim_{z \rightarrow \infty} \text{erf}(z/2) = 1$ and we have $\lim_{z \rightarrow \infty} \delta S^{(0)}(z) = 0$, as expected.

Finally, using Eq. (B.16), we obtained from Eq. (B.9)

$$\frac{\partial}{\partial z} [\eta^{(1)}(z)(\delta S^{(0)}(z) + 2)] = 2\Delta \frac{1 - N_s}{\sqrt{\pi}} \frac{\partial}{\partial z} \exp\left(-\frac{z^2}{4}\right). \quad (\text{B.21})$$

By further integration, we find

$$\eta^{(1)}(z) = \frac{\Delta \frac{1-N_s}{\sqrt{\pi}} \exp\left(-\frac{z^2}{4}\right) + A_3}{N_s + (1 - N_s) \operatorname{erf}(z/2)}, \quad (\text{B.22})$$

where we used $\lim_{z \rightarrow \infty} \delta S^{(0)} = 0$ and A_3 is an integration constant.

If we take into account image charges inside an electrode, the electric field at the infinite distance from the electrode should be zero, as explained in the main text. The $L \rightarrow \infty$ limit of z is given by $z \rightarrow \infty$ because we have $z = y/\sqrt{\tau}$, $y = x/\lambda_D$, and $x = L$. Noting that the dimensionless field is denoted by $\eta^{(1)}$, we obtained $A_3 = 0$ from Eqs. (B.22) and (12).

By substituting Eq. (B.22) into Eq. (B.15), the voltage difference was calculated as

$$V(z) = -E_0 \lambda_D \Delta \int_z^\infty dz \frac{\frac{1-N_s}{\sqrt{\pi}} \exp\left(-\frac{z^2}{4}\right)}{N_s + (1 - N_s) \operatorname{erf}(z/2)} \quad (\text{B.23})$$

$$= -E_0 \lambda_D \Delta \ln \left[N_s + \frac{1 - N_s}{\sqrt{\pi}} \int_0^{z'} dz_1 \exp\left(-\frac{z_1^2}{4}\right) \right] \Big|_{z'=z}^{z'=\infty} \quad (\text{B.24})$$

$$= E_0 \lambda_D \Delta \ln \left[N_s + (1 - N_s) \operatorname{erf}\left(\frac{z}{2}\right) \right]. \quad (\text{B.25})$$

The total voltage difference between the electrode surface and bulk was obtained from $V(0)$ as

$$V_{\text{HP}} = \frac{k_B T}{e} \frac{D_+ - D_-}{D_+ + D_-} \ln(N_s). \quad (\text{B.26})$$

Although the concentration of cations should be lower than that of anions near the electrode because of the reduction of H_3O^+ at the electrode surface, the charge neutrality condition expressed by Eq. (B.7) was obtained as the lowest-order solution from the expansion of $1/\tau$.

Conventionally, Eq. (B.26) has been derived using the difference in chemical potentials at the boundaries of liquid junctions.¹¹ In the derivation in Appendix B, we used different boundary conditions and the result indicates that the voltage change caused by electrolytic reactions at an electrode surface can be approximated by the Henderson–Planck equation in strong electrolytes.

Interestingly, the diffusion potential can be derived by assuming charge neutrality though the existence of a potential difference in principle contradicts the charge neutrality condition.¹¹ When the charges do not accumulate at the interface between the electrode and electrolyte, the positive and negative currents should be equal. The equality of the positive

and negative currents in the steady state can be expressed as

$$D_+ \left[\frac{\partial n_+}{\partial x} - \left(\frac{eEn_+}{k_B T} \right) \right] = D_- \left[\frac{\partial n_-}{\partial x} + \left(\frac{eEn_-}{k_B T} \right) \right], \quad (\text{B.27})$$

and the charge neutrality condition is given by $n_+ = n_-$. By introducing the charge neutrality condition, we obtain from Eq. (B.27)

$$E = \frac{k_B T}{e} \frac{D_+ - D_-}{D_+ + D_-} \frac{1}{n_+} \frac{\partial n_+}{\partial x}, \quad (\text{B.28})$$

and the potential difference can be obtained as Eq. (B.26).¹¹

* k-seki@aist.go.jp

- ¹ V. G. Levich, *Physicochemical Hydrodynamics*, 2nd ed. (PrenticeHall, EnglewoodCliffs,NJ, 1962) Chap. 6.
- ² J. Newman and K. E. Thomas-Alyea, *Electrochemical Systems*, 3rd ed. (John Wiley & Sons, Inc., Honoken NJ, 2004) Chap. 11.
- ³ A. J. Bard and L. R. Faulkner, *Electrochemical Methods: Fundamentals and Applications* (John Wiley & Sons, Inc, 2001).
- ⁴ S. Mafé, J. Pellicer, and V. M. Aguilera, *J. Phys. Chem.* **90**, 6045 (1986).
- ⁵ M. Bier, O. Palusinski, R. Mosher, and D. Saville, *Science* **219**, 1281 (1983).
- ⁶ R. P. Buck, *Journal of Membr. Sci.* **17**, 1 (1984).
- ⁷ H. Cohen and J. W. Cooley, *Biophys. J* **5**, 145 (1965).
- ⁸ I. Rubinstein and L. Shtilman, *J. Chem. Soc., Faraday Trans. 2* **75**, 231 (1979).
- ⁹ P. Henderson, *Z Phys Chem* **59**, 118 (1907).
- ¹⁰ E. J. F. Dickinson, J. G. Limon-Petersen, and R. G. Compton, *J. Solid State Electrochem.* **15**, 1335 (2011).
- ¹¹ J. L. Jackson, *J. Phys. Chem.* **78**, 2060 (1974).
- ¹² M. Z. Bazant, K. Thornton, and A. Ajdari, *Phys. Rev. E* **70**, 021506 (2004).
- ¹³ G. Grossman, *J. Phys. Chem.* **80**, 1616 (1976).
- ¹⁴ V. V. Nikonenko, N. D. Pismenskaya, E. I. Belova, P. Sistat, P. Huguet, G. Pourcelly, and C. Larchet, *Adv. Colloid and Interface Sci.* **160**, 101 (2010).
- ¹⁵ L.-J. Cheng and H.-C. Chang, *Biomicrofluidics* **5**, 046502 (2011).

- ¹⁶ V. I. Zabolotskii, V. V. Bugakov, M. V. Sharafan, and R. K. Chermit, *Russ. J. Electrochem.* **48**, 650 (2012).
- ¹⁷ Y. Kharkats and A. Sokirko, *J. Electroanal. Chem. Interfacial Electrochem.* **303**, 27 (1991).
- ¹⁸ C. P. Nielsen and H. Bruus, *Phys. Rev. E* **89**, 042405 (2014).
- ¹⁹ J. Jin, K. Walczak, M. R. Singh, C. Karp, N. S. Lewis, and C. Xiang, *Energy Environ. Sci.* **7**, 3371 (2014).
- ²⁰ C. Xiang, A. Z. Weber, S. Ardo, A. Berger, Y. Chen, R. Coridan, K. T. Fountaine, S. Haussener, S. Hu, R. Liu, N. S. Lewis, M. A. Modestino, M. M. Shaner, M. R. Singh, J. C. Stevens, K. Sun, and K. Walczak, *Angew. Chem. Int. Ed.* **55**, 12974 (2016).
- ²¹ R. Femmer, A. Mani, and M. Wessling, *Sci. Rep.* **5**, 11583 (2015).
- ²² Q. Wang, T. Hisatomi, Q. Jia, H. Tokudome, M. Zhong, C. Wang, Z. Pan, Z. Pan, T. Takata, M. Nakabayashi, N. Shibata, Y. Li, I. D. Sharp, A. Kudo, T. Yamada, and K. Domen, *Nat. Mater.* **15**, 611 (2016).
- ²³ Q. Wang, T. Hisatomi, Y. Suzuki, Z. Pan, J. Seo, M. Katayama, T. Minegishi, H. Nishiyama, T. Takata, K. Seki, A. Kudo, T. Yamada, and K. Domen, *J. Am. Chem. Soc.* **139**, 1675 (2017).
- ²⁴ H. Chang and G. Jaffé, *J. Chem. Phys.* **20**, 1071 (1952).
- ²⁵ L. R. Evangelista, E. K. Lenzi, G. Barbero, and J. R. Macdonald, *J Chem. Phys.* **138**, 114702 (2013).
- ²⁶ H. H. Girault, *Analytical and Physical Electrochemistry*, Fundamental Sciences (EPFL, Great Britain, 2004).
- ²⁷ N. Mott and R. Watts-Tobin, *Electrochim. Acta* **4**, 79 (1961).
- ²⁸ P. W. Debye and E. Hückel, *Phys. Z.* **24**, 185 (1923).
- ²⁹ Y. Levin, *Rep. Prog. Phys.* **65**, 1577 (2002).
- ³⁰ D. Andelman, in *Soft Condensed Matter Physics in Molecular and Cell Biology*, edited by W. Poon and D. Andelman (Taylor & Francis, New York, 2006) pp. 97–122.
- ³¹ P. Debye and H. Falkenhagen, *Phys. Z.* **29**, 121 (1928).
- ³² R. J. Silbey, R. A. Alberty, and M. G. Bawendi, *Physical Chemistry, 4th Edition* (John Wiley & Sons, New Jersey, 2005).
- ³³ D. A. McQuarrie and J. D. Simon, *Physical Chemistry: a Molecular Approach* (University Science Books, California, 1997).
- ³⁴ G. Barbero and D. Olivero, *Phys. Rev. E* **65**, 031701 (2002).

- ³⁵ K. Kontturi, L. Murtoimäki, and J. A. Manzanares, *Ionic Transport Processes: In Electrochemistry and Membrane Science* (Oxford University, UK, 2008).
- ³⁶ J. R. Bolton, S. J. Strickler, and J. S. Connolly, *Nature* **316**, 495 (1985).
- ³⁷ M. C. Hanna and A. J. Nozik, *J. Appl. Phys.* **100**, 74510 (2006).
- ³⁸ M. F. Weber and M. J. Dignam, *J. Electrochem. Soc.* **131**, 1258 (1984).
- ³⁹ M. Weber and M. Dignam, *Int. J. Hydrogen Energ.* **11**, 225 (1986).
- ⁴⁰ L. C. Seitz, Z. Chen, A. J. Forman, B. A. Pinaud, J. D. Benck, and T. F. Jaramillo, *ChemSusChem* **7**, 1372 (2014).
- ⁴¹ R. E. Rocheleau and E. L. Miller, *Int. J. Hydrogen Energ.* **22**, 771 (1997).
- ⁴² C. C. L. McCrory, S. Jung, I. M. Ferrer, S. M. Chatman, J. C. Peters, and T. F. Jaramillo, *J. Am. Chem. Soc.* **137**, 4347 (2015).
- ⁴³ C. R. Cox, J. Z. Lee, D. G. Nocera, and T. Buonassisi, *Proc. Natl. Acad. Sci. USA* **111**, 14057 (2014).
- ⁴⁴ D. A. Vermaas, M. Sassenburg, and W. A. Smith, *J. Mater. Chem. A* **3**, 19556 (2015).
- ⁴⁵ M. A.-K. Urtenov, E. V. Kirillova, N. M. Seidova, and V. V. Nikonenko, *J. Phys. Chem. B* **111**, 14208 (2007).
- ⁴⁶ J. K. Nørskov, J. Rossmeisl, A. Logadottir, L. Lindqvist, J. R. Kitchin, T. Bligaard, and H. Jónsson, *J. Phys. Chem. B* **108**, 17886 (2004).
- ⁴⁷ J. Rossmeisl, A. Logadottir, and J. Nørskov, *Chem. Phys.* **319**, 178 (2005).
- ⁴⁸ A. V. Akimov, A. J. Neukirch, and O. V. Prezhdo, *Chem. Rev.* **113**, 4496 (2013).
- ⁴⁹ T. Hisatomi, K. Takanabe, and K. Domen, *Catalysis Lett.* **145**, 95 (2014).
- ⁵⁰ Z. W. Seh, J. Kibsgaard, C. F. Dickens, I. Chorkendorff, J. K. Nørskov, and T. F. Jaramillo, *Science* **355**, 146 (2017).
- ⁵¹ L. A. Kibler, *ChemPhysChem* **7**, 985 (2006).
- ⁵² J. D. Benck, T. R. Hellstern, J. Kibsgaard, P. Chakthranont, and T. F. Jaramillo, *ACS Catalysis* **4**, 3957 (2014).
- ⁵³ Y. Jiao, Y. Zheng, M. Jaroniec, and S. Z. Qiao, *Chem. Soc. Rev.* **44**, 2060 (2015).
- ⁵⁴ N. V. Kampen, *Stochastic Processes in Physics and Chemistry* (North Holland, 2007) chapter VII. The factor 2 on the left-hand side is needed if $k_{\text{irr}}[\text{H}]^2$ represents the number of reaction events per unit time per unit volume. The factor 2 indicates that the number of molecules changed by each reaction event is equal to the difference in stoichiometric coefficients.

⁵⁵ M. Abramowitz and I. A. Stegun, *Handbook of Mathematical Functions* (Dover, New York, 1972).